The Journal of Neuroscience, January 1991, 11(1): 226–237

Chemically Distinct Compartments of the Thalamic VPM Nucleus in Monkeys Relay Principal and Spinal Trigeminal Pathways to Different Layers of the Somatosensory Cortex

E. Rausell and E. G. Jones

Department of Anatomy and Neurobiology, University of California, Irvine, California 92717

The ventral posteromedial nucleus (VPM) of the monkey thalamus was investigated with combined immunocytochemical, histochemical, and connection-tracing techniques. Injections of anterogradely transported tracers were placed selectively in the caudal nucleus of the spinal trigeminal nuclear complex, and retrogradely transported horseradish peroxidase (HRP) or fluorescent dyes were placed on the surface or into the depths of defined parts of the trigeminal representation in the first somatic sensory area (SI) of the cerebral cortex. The results are correlated with those of the preceding paper (Rausell and Jones, 1991), which demonstrated the presence of 2 domains in the nucleus on the basis of different patterns of cytochrome oxidase (CO) staining and calcium-binding protein immunoreactivity.

The cells of the CO-defined rod and matrix domains receive inputs from different components of the trigeminal afferent system and project to different layers of SI. The large- and medium-sized relay cells of the CO-rich rods, which are immunoreactive for parvalbumin, all project to middle layers of SI. The small relay cells of the weakly-stained CO-matrix, surrounding and intervening between the rods, are immunoreactive for 28-kDa calbindin and project to superficial layers (I and II) of SI.

Anterograde tracing studies reveal that the rod domain in VPM is innervated by fibers arising in the contra- and ipsilateral principal trigeminal nucleus, while the matrix domain (and calbindin-positive domains in adjacent nuclei) are innervated by fibers arising in the caudal nucleus of the spinal trigeminal complex.

These results demonstrate the modularity and parallel streaming of the functional components of the trigeminal part of the somatic sensory system and suggest that lemniscal and nonlemniscal elements of the system gain access by separate routes to different layers of the SI cortex.

In a companion paper (Rausell and Jones, 1991) and in our previous studies (Jones et al., 1986a,b), it has been demonstrated that the ventral posterior medial nucleus (VPM) of the monkey thalamus is divided into histochemically and immunocytochemically distinct compartments. One of these, the cytochrome oxidase- (CO) rich *rod domain,* contains cells immunoreactive for the calcium-binding protein, parvalbumin, and for a surface proteoglycan identified by the monoclonal antibody, CAT 301. It shows a high degree of modular organization of place- and modality-specific cells similar to that demonstrable at other levels of the lemniscal component of the somatic sensory pathways (Mountcastle, 1984). The second compartment, the CO-weak *matrix domain,* is selectively immunoreactive for another calcium-binding protein, 28-kDa calbindin, and is CAT 301 negative. It has not yet been physiologically characterized. However, it is known that both parvalbumin- and calbindin-immunoreactive cells in VPM and other nuclei project to the cerebral cortex (Jones and Hendry, 1989). Therefore, the 2 compartments of VPM may represent separate channels for afferent inputs to the somatic sensory cortex (SI), and it becomes important to ascertain their input–output relations.

The rod compartment has already been shown to be the terminus of fibers from the principal trigeminal nucleus (Jones et al., 1986b), and elongated rods of cells in VPM were previously demonstrated to have the same place and modality properties and to project to focal domains in the first somatic sensory area (SI; Jones et al., 1982). These are properties commensurate with the parvalbumin-immunoreactive cells of the VPM rods forming the relay for the lemniscal component of the trigeminal system. The question, therefore, arises as to whether the calbindin-immunoreactive cells of the VPM matrix form the relay for nonlemniscal components.

Recent studies in primates indicate the presence of both nociceptive-specific and other types of responding cells and fibers throughout the successive levels of the spinothalamic pathway and its companion system arising in the caudal nucleus of the spinal trigeminal complex (Willis et al., 1979; Chung et al., 1986a,b; Willis, 1987; Surmeier et al., 1988; Yezierski et al., 1988). In cats, there are indications of a nociceptive-specific part of the thalamus which adjoins the rest of the ventral posterior nuclear complex, and which includes a trigeminal component (Kniffki and Mizumura, 1983; Kniffki and Vahle-Hinz, 1987; Vahle-Hinz et al., 1987; Yokota et al., 1983, 1985, 1988). Further work is therefore required to determine whether these findings betoken the presence of routes to the cerebral cortex parallel to, but separate from, the lemniscal system and whether they are reflected in the different histochemical and immunocytochemical properties of the relevant cells and relay centers.

In the present study, CO histochemistry and calcium-binding protein immunoreactivity have been combined with anatomical

Received June 12, 1990; revised Aug. 30, 1990; accepted Sept. 5, 1990.

This work was supported Grants NS21377 and NS22317 from National Institutes of Health, U.S. Public Health Service. E.R. was the recipient of a Fullbright Fellowship and a Fogarty International Fellowship. We thank Dr. P. C. Emson for the parvalbumin and calbindin antisera and Dr. C. Matute and Dr. P. Streit for the GABA monoclonal antibody.

Correspondence should be addressed to Dr. E. G. Jones. Department of Anatomy and Neurobiology, University of California, Irvine, CA 92717.

tracing techniques to reveal the selective channeling of the lemniscal and caudal trigeminal inputs through the monkey thalamus en route to the cerebral cortex by means of chemically distinct populations of cells.

A preliminary report has previously appeared (Rausell and Jones, 1989).

Materials and Methods

The experiments were carried out on 23 adult cynomolgous monkeys (*Macaca fascicularis*), weighing 3.0–3.5 kg. Ten normal monkeys, which had also been used in the accompanying study (Rausell and Jones, 1991) were used for immunocytochemistry. Eight others were used for combined immunocytochemical and tracing studies, and 5 were used in anterograde and retrograde tracing studies alone. Material from earlier studies involving 10 additional monkeys with small injections of horseradish peroxidase at physiologically defined sites in the SI cortex (Jones et al., 1982) was also examined.

Double-labeling and retrograde-labeling studies. In 8 monkeys, bilateral craniotomies were performed over the lateral third of both left and right postcentral gyri, under intravenous Nembutal anesthesia and aseptic conditions. On the left side, penetrations with a tungsten or stainless-steel microelectrode were made in the first somatic sensory area (SI), in a region close to the lateral end of the central sulcus, in order to locate and partially map by means of multiunit recording the cortical region containing the representation of the face. In 6 animals, upon identification of a region containing neurons responding to tactile stimulation of the contralateral or ipsilateral side of the mouth, the recording electrode was replaced by a micropipette with a tip diameter of 20–50 μm and filled with 5% fast blue. This was lowered to a depth of 1–1.5 mm, and 0.1–0.2 μl was injected at this and at 2–4 surrounding sites by air-pressure pulses. On the right side, an approximately corresponding cortical region was located visually, but electrode penetrations were not made in it. An area approximately 1 cm^2 was gently rubbed with cotton that had been soaked in 0.1 M acetate buffer (pH, 2.5) until hyperemia was detected at the cortical surface. Then, a piece of filter paper, previously soaked in 5% fast blue solution, was applied to the cortical surface. After 10 min, it was removed and replaced with a second that was left in place. The animals survived for 2 weeks. After that period, they were deeply anesthetized with intravenous Nembutal and perfused with 4% paraformaldehyde and 0.2% glutaraldehyde in 0.1 M phosphate buffer. All brains were removed, infiltrated with 30% sucrose, frozen in dry ice, and sectioned on a sliding microtome.

In the remaining 2 animals, a portion of the face representation was first identified by microelectrode recording as above. Then, a micropipette with a tip diameter of 20 μm and containing 20% horseradish peroxidase (HRP; Sigma type VI) in normal saline was returned to one of the tracks and lowered to a depth of 1 mm, and 0.02–0.05 μl was injected by air pressure. The 10 other brains from the earlier study also involved HRP injections of this type.

The thalami from the brains injected with fast blue were cut into a series of frontal sections in which 5 15-μm sections alternated with 1 30-μm section. The first of each group of 6 sections was mounted quickly for immediate examination of the thalamic cells retrogradely labeled with fast blue. The adjacent 30-μm section was stained with 0.25% thionin or cresyl violet. The remaining 15-μm sections were stained immunocytochemically using the same primary antisera as in the previous paper (Rausell and Jones, 1991). They were incubated for 36–48 hr at 4°C in antiparvalbumin antiserum (1:5000), in anti-calbindin antiserum (1:2000), or in both of these together, made up in 0.1 M phosphate buffer containing 5% normal serum from the species in which secondary antibodies were made but without the addition of Triton X-100. After repeated washing in phosphate buffer, they were further incubated for 2 hr at 4°C in solutions without Triton, and containing fluorescein isothiocyanate-conjugated donkey anti-goat or anti-sheep (for parvalbumin) or rhodamine isothiocyanate-conjugated donkey anti-rabbit (for calbindin) secondary immunoglobulins (Chemicon), or in both of these together, each diluted 1:200 in 0.1 M phosphate buffer and 5% normal serum. Other sections containing fast blue-labeled cells were similarly incubated in the same anti-GABA monoclonal antibody or antiserum as in the previous paper (Rausell and Jones, 1991), but also without Triton, followed by fluorescein-conjugated goat anti-mouse or goat anti-rabbit secondary immunoglobulins exactly as described in the previous paper. After further washing, all sections were mounted under coverslips on cleaned slides in 0.1 M phosphate-buffered glycerol (1:3). They were examined immediately for fast blue and immunofluorescence, using a Leitz Dialux epifluorescence microscope equipped with wideband ultraviolet, rhodamine, and fluorescein filter packs. Cytochrome oxidase (CO) histochemistry (Wong-Riley, 1979) or thionin staining was carried out on alternating 30-μm-thick sections. Immunocytochemical controls were as reported in Rausell and Jones (1991).

In the brains injected with horseradish peroxidase, the thalami were cut serially at 50 μm in the frontal plane, and every section was reacted by the Mesulam (1981) or Hardy and Heimer (1977) protocol. Every other reacted section was later counterstained with thionin.

Camera lucida drawings of both the fluorescence and the HRP material were made at high and low magnification, and all neurons labeled with fast blue or horseradish peroxidase or by immunostaining and found in the VPM nucleus were plotted on them. The Nissl-stained sections were then used for precisely outlining the borders of the nucleus, and the CO sections were used for outlining the limits of the CO-stained rod and matrix domains found in VPM. Drawings of each type were later superimposed, using the outlines of the same sectioned blood vessels as guides.

Anterograde tracing. In 3 monkeys, anesthetized by intravenous Nembutal and under aseptic conditions, the neck muscles were detached from the occipital bone on one side to expose the atlanto-occipital membrane. This was incised, the cisterna magna was opened, and a tungsten microelectrode was introduced into the lateral part of the medulla oblongata on one side. One to 3 penetrations were used to identify and localize the caudal subnucleus of the spinal trigeminal complex by recording neuronal responses to light mechanical stimulation of the ipsilateral side of the head, face, and mouth. Thereafter, the microelectrode was withdrawn and replaced by a micropipette with a 20-μm tip and containing a mixture of 20% type VI horseradish peroxidase (Sigma) in 1% wheat germ agglutinin-conjugated horseradish peroxidase (Sigma) in 0.1 M Tris-buffered saline. Two to 4 μl of this mixture was injected at 1 or 3 sites by means of an oil-filled hydraulic system coupled to the pipette.

After a survival time of 48 hr, these animals were deeply anesthetized and perfused with a mixture of 1% paraformaldehyde and 2% glutaraldehyde in 0.1 M phosphate buffer, followed by 10% phosphate-buffered sucrose. The brains were further infiltrated with sucrose, then blocked and sectioned serially at 50 μm on a freezing microtome. The diencephalon was cut in the frontal plane, and the brain stem was cut in a plane transverse to its longitudinal axis. Alternate sections were reacted for horseradish peroxidase by the Mesulam (1978) protocol or for CO. The distribution of anterogradely labeled fibers was plotted on camera lucida outlines of VPM, which were then superimposed on similar drawings showing the distribution of CO staining in the adjacent section. These data were compared with data derived from our previously published anterograde tracing experiments that involved injections of horseradish peroxidase in the principal trigeminal nucleus (Jones et al., 1986b).

Results

Small HRP injections in the SI face representation

Figure 1 is representative of experiments from the present and past series (Jones et al., 1982) that involved tiny injections of HRP at sites of known representation in the face area of SI. In the case illustrated, the injection was made into a microelectrode track in which units with receptive fields in the ipsilateral cheek pouch were recorded. The injection is less than 1 mm in horizontal extent, is restricted to area 3b, and involves layers I–IV only.

Most retrogradely labeled cells in the thalamus are confined to an elongated region extending through much of the anteroposterior extent of the horizontal part of the VPM. In a single section, relatively few cells are labeled, and they form a cluster of some 20–30 cells (Figs. 1, 2). This cluster correlates very closely with a clump of large Nissl-stained cells and with the rodlike patch of CO staining seen regularly at this site and in the position in which the cheek pouch is usually represented (see Rausell and Jones, 1991; their Fig. 8). More posteriorly in the nucleus, labeled cells may encroach upon the region in which

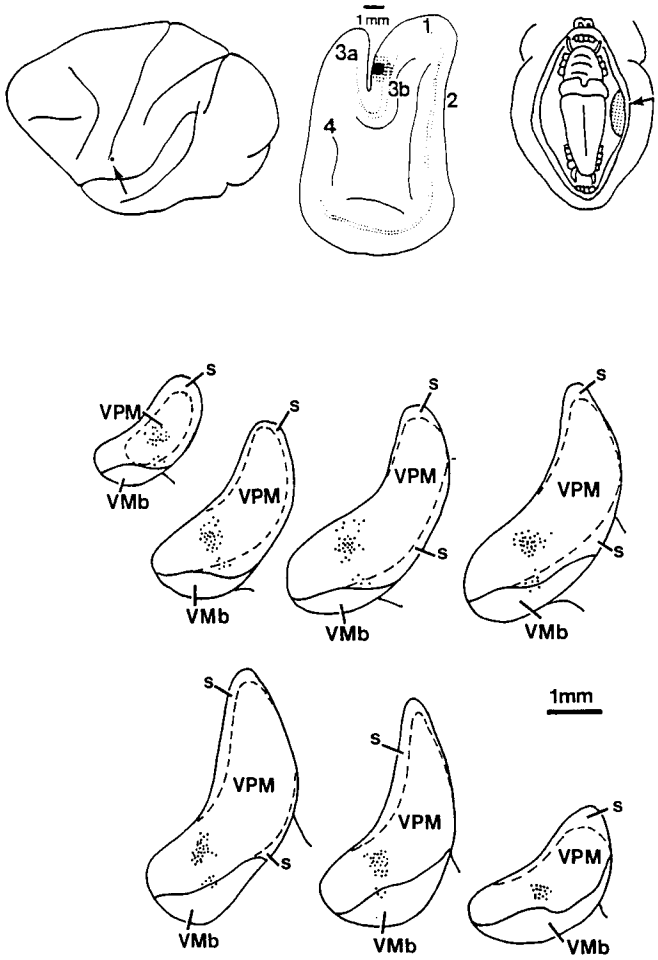

Figure 1. Camera lucida drawings of series of a frontal sections in anterior (*top left*) to posterior (*bottom right*) order. This figure shows the distribution of retrogradely labeled cells in an anteroposteriorly elongated array in the rod domain and scattered in the matrix (*s*) domain (*arrows*) in an animal in which a small, focal injection of HRP (*top left* and *middle*) was made at a site in SI in which the ipsilateral cheek pouch (*top right*) was represented.

the tongue and floor of the mouth are represented, presumably reflecting injection spread in the cortex.

In addition to the medium- and large-sized cells that are retrogradely labeled in the region corresponding to the representation of the ipsilateral cheek pouch, a group of small retrogradely labeled cells is seen over part of the anteroposterior extent of the others. These small cells are few in number and extend away from the retrogradely labeled rodlike region into the small-celled region adjacent to the ventral medial basal nucleus (VMb), which is characterized as a region of weak CO staining and which forms part of the matrix domain (Figs. 1, 2).

In reevaluating material from our previously published experiments involving similar small injections of HRP at physiologically defined sites in the face area of SI, 2 things are clear: The smallest injections retrogradely label large- and medium-sized cells in a single, long narrow rod stretching anteroposteriorly through VPM (see Jones et al., 1982, their Fig. 3), and occasional small labeled cells are regularly seen adjacent to the larger labeled cells, as in Figure 2.

Double-labeling experiments

Fast blue injections in SI

The large, deep injections of fast blue in SI were, in all animals, located in area 3b, as revealed by Nissl staining. They are much larger than the HRP injections described above. On the contralateral side, the superficial deposits of fast blue strongly affected layer I, with a little tracer spreading to layer II but not deeper. The extent of both types of injections was approximately 3 mm^2 (Figs. 3–6).

VPM projections to middle and deep layers of the SI face area

Fast blue injections involving all layers of the SI cortex, located in the face or mouth representation, resulted in retrograde labeling of neurons in VPM. In one representative case (CM 264; Fig. 3), the tracer was injected in regions of the SI cortex, where neurons had receptive fields on the skin of the contralateral lower jaw, chin, and lower lip, but it clearly spread to adjacent regions. Retrogradely labeled neurons are concentrated in the vertical region of VPM, near the junction of this region with the horizontal region. Most of the neurons were located in clusters that, on comparison with the CO-stained sections, would form parts of the CO-stained rods but with others in the intervening matrix domain. Comparison with the multiunit map of this part of VPM showed that the position of the labeled region corresponded to that in which the neurons would be expected to have receptive fields comparable to those of neurons at the injection site and in surrounding regions to which the fast blue had spread. In a second case (CM 259; not illustrated) the receptive fields of neurons at the site of the injections were on the ipsilateral lower lip, lower teeth, and lower gum. The retrogradely labeled neurons were located in the horizontal region of VPM, grouped in several clusters 200–700 μm in diameter, which included several CO rods in the adjacent, histochemically stained sections.

The labeled cells in the rod domain in all experiments of this type are of large and medium size, and in the sections costained for immunofluorescence, clearly also show immunoreactivity for parvalbumin (Fig. 4). This is true for virtually every fast blue-labeled cell found in a region corresponding to a CO rod as seen in the adjacent section. No fast blue-labeled neurons in the rod domain, however, show costaining for calbindin. In sections costained for GABA immunofluorescence, no fast blue-containing cells are stained for GABA (Fig. 4*C*). Fast blue-labeled projection neurons within the rod domain tend to occupy separate clusters from those occupied by GABA neurons, but GABA-positive processes and puncta invade the clusters of projection neurons and outline the fast blue-labeled cells (Fig. 4*C*).

In each of the experiments involving large fast blue injections affecting all cortical layers, another small group of fast blue-labeled projection neurons can be seen outside the rod domain and within the region corresponding to the CO matrix domain (Fig. 3). These neurons are small in size, do not show immunoreactivity for parvalbumin, and are sparsely distributed, though they tend to concentrate in clusters. In the experiment involving the contralateral representation of the face, the majority of the cells are in the dorsomedial part of the matrix (Fig. 3). In the experiment involving an injection in part of the ipsilateral face representation, they are in the ventral part (not illustrated). All of the labeled small neurons of the matrix domain also show immunoreactivity for calbindin in double-stained

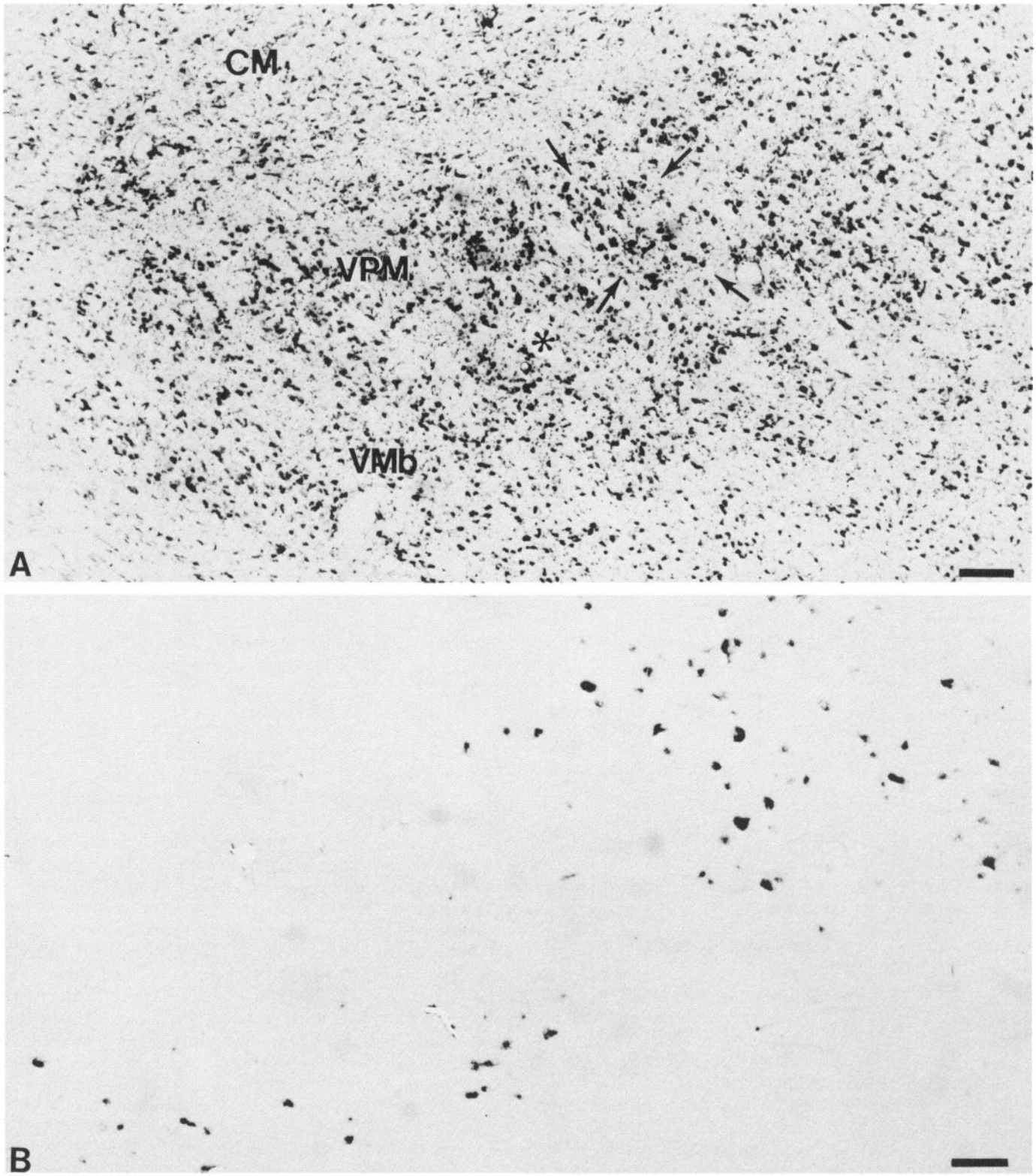

Figure 2. Adjacent counterstained (*A*) and noncounterstained (*B*) sections showing HRP labeling in rod and small-celled regions in experiment illustrated in Figure 1. The labeled cluster of cells at the *top right* in *B* is from the region *arrowed* in *A*. Labeled small cells at the *bottom left* in *B* are from small-celled region indicated by the *asterisk* in *A*. Scale bars: 250 μm, *A*; 750 μm, *B*.

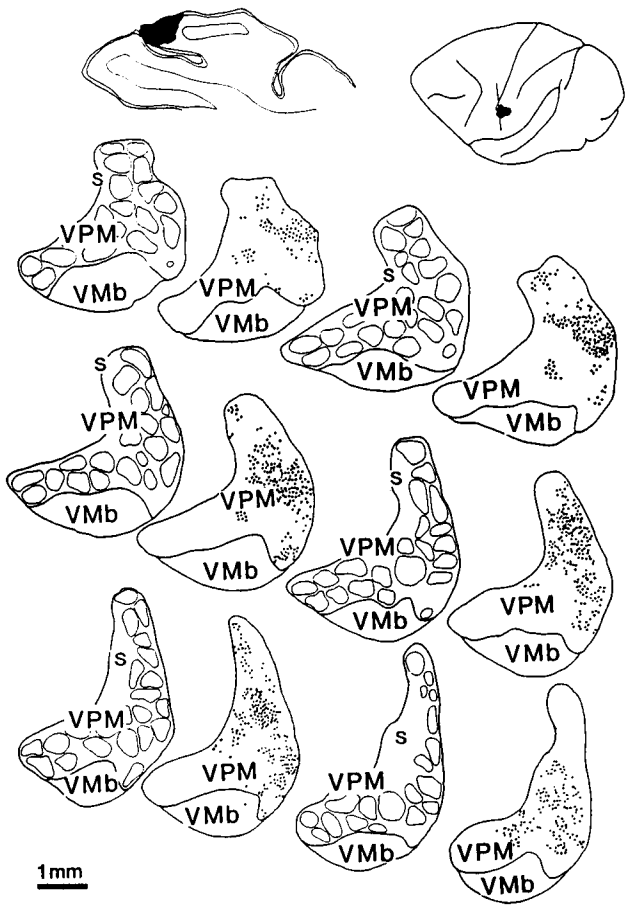

Figure 3. Pairs of adjacent sections in anterior (*top left*) to posterior (*bottom right*) order, stained for CO (*left* member of each pair) or unstained to show cells retrogradely labeled with fast blue (*right* member of each pair) following injection (*top*) of dye in contralateral face representation in SI, and which affected all cortical layers. Superimposition of the sections reveals presence of retrogradely labeled cells (*dots*) in both rod and matrix domains.

sections (see below). No fast blue-labeled cells in the matrix domain are double stained for GABA.

VPM projections to layer I of the SI face area

The superficial deposits of fast blue in the face area of SI also resulted in retrograde labeling of neurons in VPM (Fig. 5). The labeled cells are small to medium in size and are only distributed in regions corresponding to the matrix CO domain as seen in adjacent sections. They are found throughout most of the thin envelope surrounding individual rods, and particularly in the posteromedial enlargement and in the lateral and ventral convexity. Double labeling confirms that these retrogradely labeled cells are located in the calbindin-positive region and are double stained for calbindin immunoreactivity (Fig. 7). None of the fast blue-labeled, calbindin-positive cells, however, also shows immunoreactivity for parvalbumin.

In the animal in which the superficial deposit of fast blue resulted in retrograde labeling of the contralateral representation of VPM, a larger number of small, fast blue- and calbindin-positive neurons was found in the dorsomedial parts of the matrix, and they were less abundant in the ventrolateral region (Fig. 5). In the animal in which the ipsilateral representation in VPM was labeled, the greater number of small, calbindin-positive neurons was located in the ventrolateral region (not illustrated).

Anterograde-labeling experiments

Spinal trigeminal nucleus

The injection sites in the 3 brains are centered in the caudal subnucleus of the spinal trigeminal complex (Fig. 8) and extend from approximately the level of the obex to the first spinal segment. The injections are large, fill the cross-sectional extent of the spinal nucleus at these levels, and spread medially into the adjoining reticular formation from which trigeminothalamic fibers are also known to arise. In 2 brains, the deep aspect of the cuneate nucleus is affected. As a consequence of the latter, labeled ascending fibers can be detected in the contralateral medial lemniscus as well as in the regions adjacent to it throughout its length, and some labeling of terminal ramifications appears in the ventral posterior lateral nucleus (VPL) in addition to that in VPM.

Labeled fibers leaving the injected spinal trigeminal nucleus ascend both ipsi- and contralaterally towards the thalamus. Those crossing the midline do so by traversing the central gray low in the medulla and accumulate ventral to the medial lemniscus and dorsal to the pyramid. Here, they ascend, and as the lemniscus moves laterally, they are drawn into a flat sheet extending from the ventral aspect of the lemniscus to the raphe. In the midbrain, this sheet divides into medial and lateral groups of fibers, the lateral group of which ascends diffusely along the medial lemniscus to the diencephalon. The medial group consists of fibers that appear to terminate mainly in the midbrain. Fibers ascending ipsilaterally do so in much smaller numbers in the same general position.

Contralateral to the injection, very large numbers of fine, labeled fibers enter the posterior aspect of the thalamus diffusely from the field of Forel and thalamic fasciculus (Fig. 8). Most of the fibers reach VPM from the ventral direction, either penetrating it or ascending over its posterior surface to enter both the vertical and horizontal parts of the nucleus. A minority of fibers enters medial to VPM, ascends through the centre médian nucleus (CM), and then either turns laterally towards VPM, or continues towards the central lateral nucleus (CL). The posterior pole of the VPM is embedded in a sheet of fine, labeled fibers containing small dispersed patches of labeled terminal ramifications (Figs. 8, 9). Patches are seen in the posterior (Po), suprageniculate (SG), and magnocellular medial geniculate (MGmc)

→

Figure 4. Fluorescence micrographs of identical field from same triple-stained section from *VPM* (*asterisks* indicate same landmarks), showing part of rod domain and adjoining (*top left*) portion of matrix domain. Fluorescein immunofluorescence for parvalbumin (*A*) reveals dense cell and fiber labeling in the rod domain, and fast blue fluorescence (*B*) shows that most of the parvalbumin-labeled cells of *A* are retrogradely labeled with fast blue, transported from an injection affecting middle and deep layers of the SI face area. *C*, showing rhodamine immunofluorescence for GABA, reveals the dense GABA-stained neuropil of the rod domain, lack of colocalization of GABA with parvalbumin or fast blue in cell somata, and the tendency for GABA cells to cluster between parvalbumin cells (cf. regions indicated by *arrows* in *A* with the same regions in *C*). Scale bar, 50 μm.

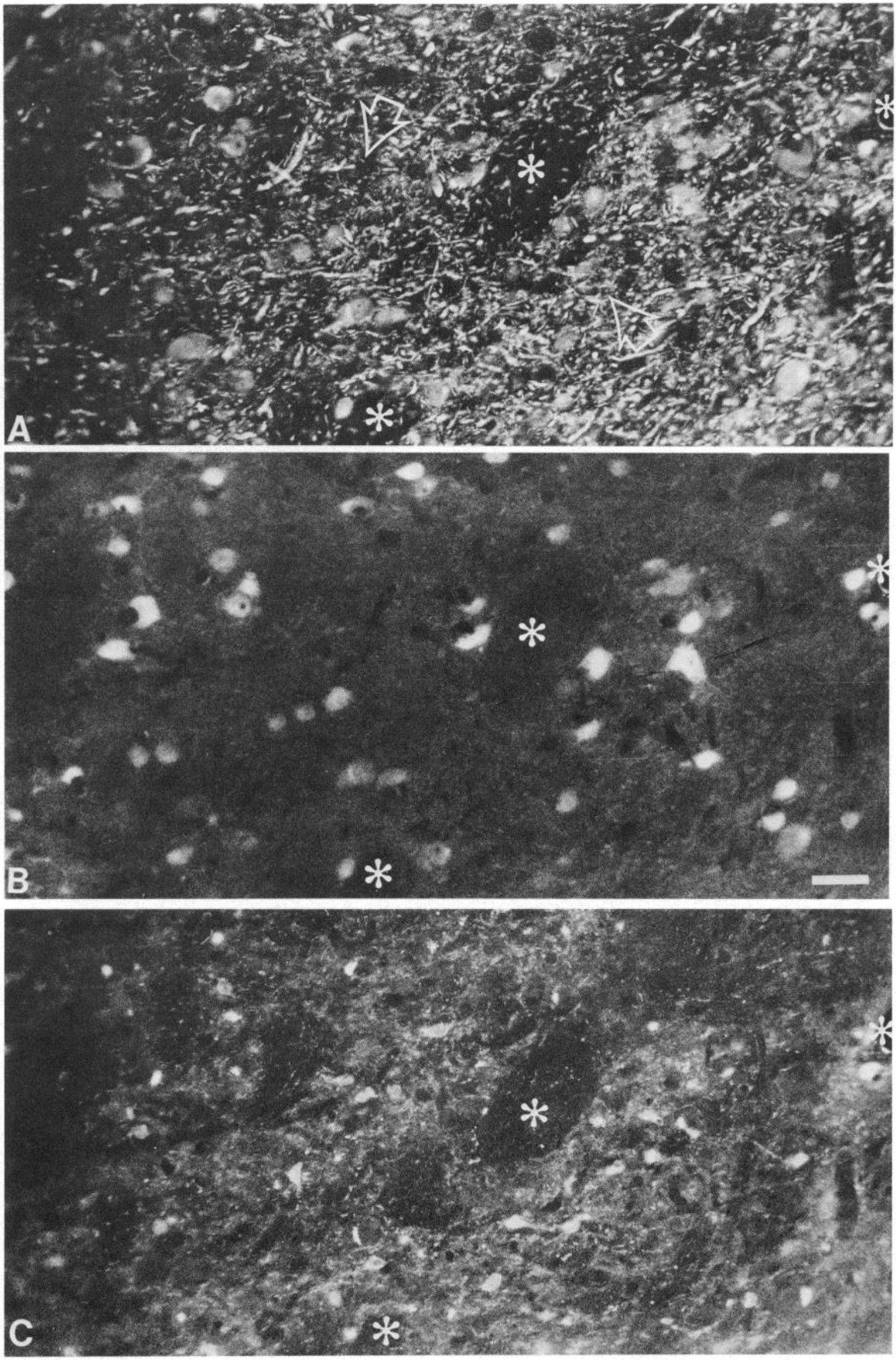
A
B
C

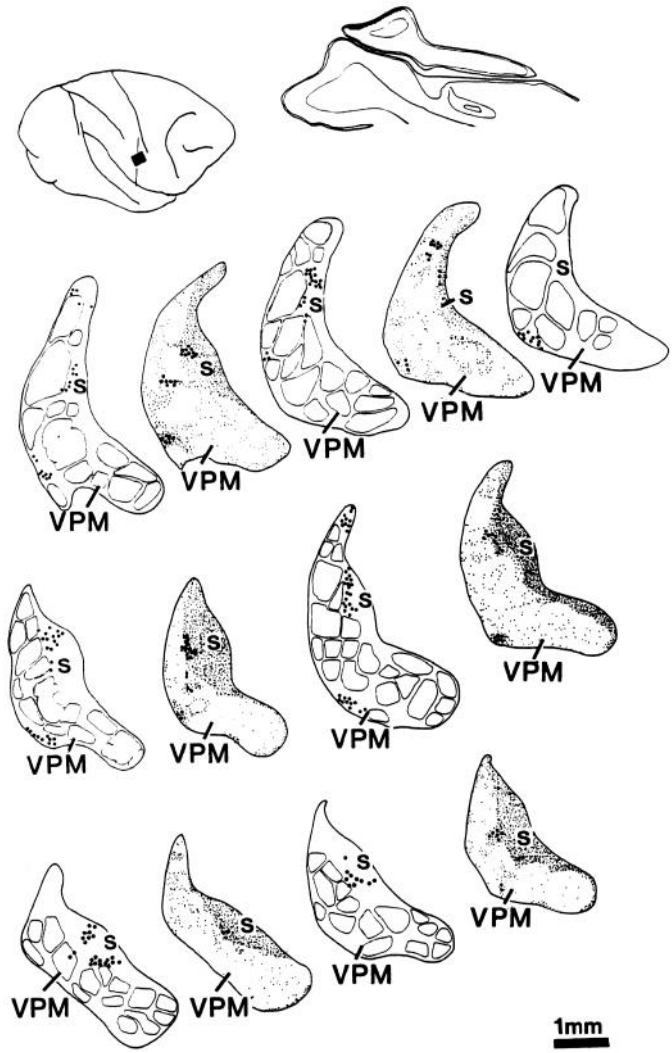

Figure 5. Pairs of adjacent sections in anterior (*top right*) to posterior (*bottom left*) order. The *right* member of each pair was stained by immunofluorescence for parvalbumin, and the drawing was superimposed on a drawing of the adjacent CO-stained section (rods indicated by *outlines*); the *left* member was stained by immunofluorescence for calbindin. Both show distribution of cells (*large dots*) retrogradely labeled with fast blue from an injection that involved layer I of the contralateral face representation in SI. Note the restriction of retrogradely labeled cells to small-celled (*s*), nonparvalbumin- but calbindin-immunoreactive (*fine stippling*) matrix region.

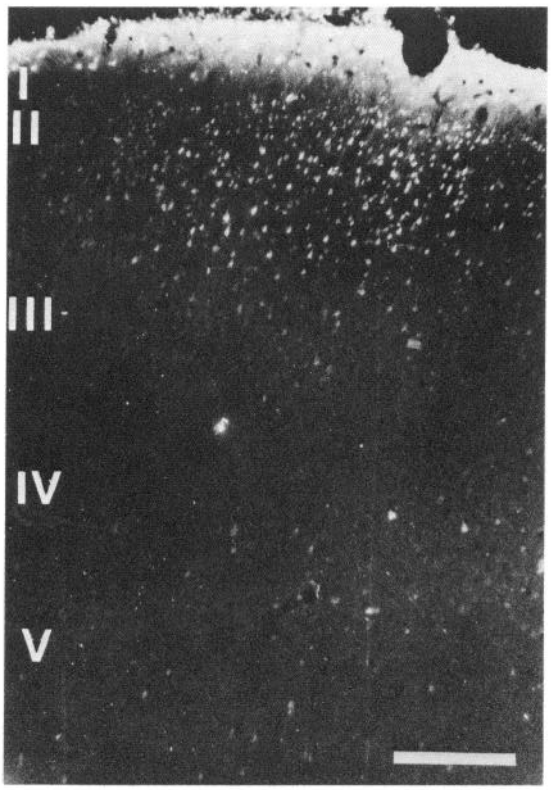

Figure 6. Fluorescence micrograph of part of section showing maximal depth of penetration of superficial deposit of fast blue of type that leads to retrograde labeling of calbindin-positive cells in matrix domain of VPM. Cells labeled in layers II–III probably incorporate fast blue via their dendrites in layer I. Scale bar, 200 μm.

nuclei. Immediately anterior to these levels, the posterior pole of VPM shows similar patches, and labeled fibers ascending over the posterior surface of VPM and over and through CM end in dense separated patches in the CL and anterior pulvinar (Pla) nuclei. A large number of labeled fibers can also be seen ascending in the lamina separating the Pla from VPM.

Most of the posterior ⅔ of VPM is encased in fine, labeled fibers, which outline its borders and those of the ventral medial basal nucleus (VMb; Figs. 8, 9). No fibers appear to terminate in VMb, though a few pass through it. By contrast, many regions corresponding to the CO-weak matrix zones of VPM, as determined from the alternate, CO-stained sections, are permeated by fine, labeled fibers with interspersed patches of terminal ramifications. Labeled fibers and terminal patches are absent from most of the medial ⅔ of the horizontal part of VPM but fill the part corresponding to the CO-weak matrix regions at the posterior pole, at the ventrolateral expansion, and between the CO rods of the contralateral representation. Posteriorly, they encroach on a region corresponding to the most medially placed rods (Figs. 8, 9*A*).

On passing anteriorly, regions corresponding to the CO-weak matrix in the dorsomedial concavity and over the dorsal surface of the vertical part of VPM, as well as to the matrix between the CO rods, also show permeation by fine, labeled fibers and contain occasional terminal patches (Figs. 8, 9). Of special note is the presence of 4 or 5 unusually dense patches of labeled terminal ramifications in part of the CO rod region (Figs. 8, 9*B*, arrows). These measure from 100 to 300 μm in diameter, but none is sufficiently large to fill the mediolateral extent of a rod. Two or 3 of the larger patches are found around large cells that form parts of rods situated in the contralateral representation close to the border with the ipsilateral representation, probably in the representation of the tongue and cheek (Rausell and Jones, 1991), but only in the posterior ⅓ of the nucleus. Three or 4 smaller clusters are found around large cells in the medial edges of rods close to the border with Pla and CM, but only in the middle and anterior thirds of VPM. These clusters are very similar to those seen in CL; a number of clusters also appear in the anterior part of Pla where it abuts on the medial matrix of VPM (Figs. 8, 9*C*).

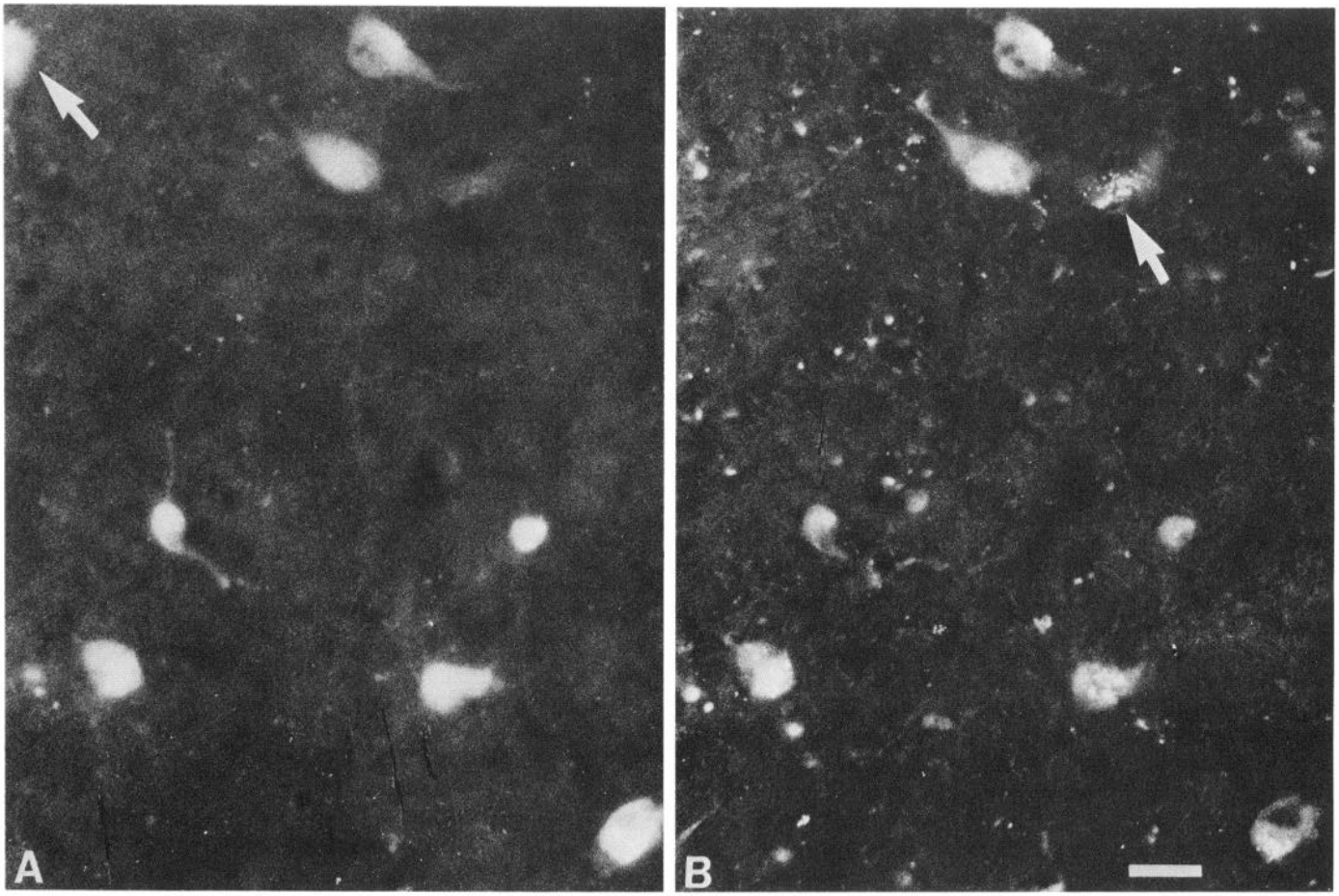

Figure 7. Fluorescence micrographs of same field from matrix domain, showing small calbindin-immunoreactive cells (*A*) identified by fluorescein immunofluorescence and many of the same cells (*B*) retrogradely labeled with fast blue from injection involving layer I of SI face area. Cells that are *not* double labeled are indicated by *arrows*. Scale bar, 20 μm.

Ipsilateral to the injection site, a few labeled fibers enter the thalamus along a trajectory similar to that seen on the contralateral side. A few patches of terminal label can be seen in CL and medially at the posterior pole of VPM.

Principal trigeminal nucleus

The ascending course of fibers from the principal trigeminal nucleus and their terminal distribution in the ipsi- and contralateral thalamus have been previously described and illustrated (Jones et al., 1986b; their figs. 2, 3). Here, only the details of the terminal patterns will be described.

All labeled fibers ascending from the principal trigeminal nucleus terminate only in the ipsi- and contralateral VPM nuclei. On the relevant sides, their terminal ramifications fill only those parts of the nucleus corresponding to the ispi- and contralateral representations. By contrast with the pattern of labeling seen after injections in the spinal trigeminal nucleus, the terminal labeling forms large, dense clusters that conform in size to the CO rods, extend anteroposteriorly through the full extent of VPM, and are exactly superimposable on the rods seen in adjacent sections stained for CO. The matrix regions at the posterior pole, dorsomedial concavity, and ventrolateral expansion are completely free of terminal labeling, and few or no labeled fibers pass through them. Scattered fine, labeled particles are found in the matrix regions between the densely labeled rods, but their density is low.

Discussion

The present results indicate that the histochemically and immunocytochemically distinct compartments of the VPM nucleus of the monkey thalamus (Rausell and Jones, 1991) can also be distinguished on the basis of differential input–output relationships. The CO-dense, parvalbumin- and CAT 301-positive *rod domain,* from the present and previous results (Jones et al., 1982, 1986a,b), clearly represents the route through which place- and modality-specific information of the classical lemniscal type is relayed to layers of SI that include the middle and deeper layers. The CO-weak, calbindin-positive, and CAT 301-negative *matrix domain,* from the present results, appears to be a likely route through which nonlemniscal information, including pain and temperature information from the head, face and mouth, would be relayed to superficial layers of SI.

The CO-dense, parvalbumin-positive rod compartment of VPM has previously been shown to be the terminus of afferents from the principal trigeminal nucleus (Jones et al., 1986b). The mapping studies reported by Rausell and Jones (1991) and in our earlier papers confirm the place and modality specificity of the rod domain, and the retrograde labeling studies of the pres-

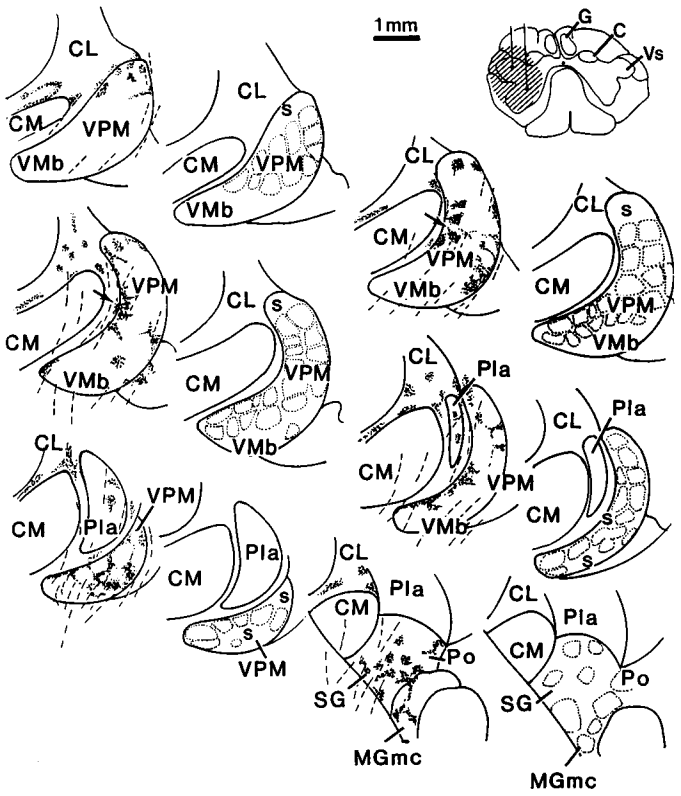

Figure 8. Camera lucida drawings of pairs of sections in anterior (*top left*) to posterior (*bottom right*) order, showing distribution of anterogradely labeled fibers and terminal ramifications (*dots*) in VPM and its vicinity (*left* member of pair) and distribution of CO-stained rods and matrix (*s*; *right* member of pair), following injections of mixed HRP and wheat germ agglutinin-conjugated HRP in the contralateral caudal nucleus of the spinal trigeminal complex and underlying reticular formation (*top right*). Note the major distribution of terminations in matrix regions of VPM and in adjoining nuclei. *Arrows* indicate where terminations intrude on the rod domain.

ent and previous studies (Jones et al., 1982; 1986b) confirm the projection of rodlike arrays of cells in VPM to focal domains in the SI cortex. These are indications of the modularity to be anticipated from the trigeminal equivalent of the dorsal column–lemniscal system (Dykes, 1983; Mountcastle, 1984).

The CO-weak, calbindin-positive matrix compartment of VPM, from the present results, seems to be the major terminus of fibers ascending to VPM from the caudal nucleus of the spinal trigeminal complex and from subjacent reticular cells that appear to be part of the trigeminal system (Price et al., 1976). Retrograde labeling studies have previously shown that the superficial layers of this nucleus and the adjoining parts of the reticular formation, as injected in the present study, project to VPM (Price et al., 1976; Burton and Craig, 1979). However, the terminations of fibers arising from the caudal nucleus, unlike those of the fibers arising from the principal nucleus that terminate only in the rod compartment, extend into relatively CO-weak, small-celled, calbindin-positive regions in the VPI, VMb, and Pla nuclei adjacent to VPM and also into several other adjacent nuclei such as CL, Po, SG, VLp, and the central medial nucleus (CeM). This widespread distribution pattern is comparable to that described with axonal degeneration methods in the squirrel monkey by Ganchrow (1978). It also has a character similar, both in its extent and in its patchy terminal pattern, to that of the spinothalamic tract terminations demonstrated in the monkey, cat, and raccoon by Burton and Craig (1983) and Craig and Burton (1985). The spinothalamic tract also terminates in VPL, which for obvious reasons contained no terminal labeling that could not be attributed to involvement of the cuneate nucleus in the present study. It is noteworthy that all the nuclei containing caudal trigeminal or spinothalamic terminals contain significant populations of calbindin-positive cells, either as their total cell population or arranged in small clusters among larger populations of parvalbumin-positive cells (Jones and Hendry, 1989; Rausell and Jones, 1991).

The spinal trigeminal fibers display some selectivity of termination in the matrix compartment in that fibers from the contralateral side end dorsolaterally, and the few from the ipsilateral side end posteromedially in the appropriate representations in VPM. Although they have a generally diffuse pattern of distribution, there are foci of terminal ramifications similar to those in adjacent nuclei. For unknown reasons, 2 or 3 of these foci seem to select portions of the rod domain in the representation of the contralateral side of the tongue and cheek, while the majority are confined to the matrix. This could imply selective convergence of principal and caudal nucleus inputs on a small population of rod cells. For technical reasons outlined in the accompanying paper (Rausell and Jones, 1991), it has not yet been possible to obtain information about the receptive fields and stimulus–response properties of neurons in the matrix domain of VPM. We might anticipate, however, that they would display features similar to those described by Price et al. (1976) in the caudal spinal trigeminal nucleus and its underlying, large, VPM-projecting cells. One group of these shows responses to light touch or pressure, others are specifically responsive to noxious thermal and mechanical stimuli, while others show mixed responses and resemble the wide dynamic range of cells of the spinothalamic system (Surmeier et al., 1988).

The presence of a small-celled matrix region that is, at its widest extent, around the dorsomedial and ventrolateral borders of VPM, and which is clearly selectively innervated by fine fibers arising from a nucleus in which nociceptive- and thermal-sensitive neurons are located, raises parallels with studies of nociceptive trigeminal cells in the thalamus of cats. In cats, Kniffki and Mizumura (1983), Kniffki and Vahle-Hinz (1987), Vahle-Hinz et al. (1987), Yokota and Matsumoto (1983), and Yokota et al. (1985, 1988) have shown that such cells are preferentially located in a shell-like region around VPM. In the studies of Yokota et al. (1988), this shell is described as part of a wider nociceptive zone for the body extending laterally around VPL, as well. The dorsally situated nociceptive cells of VPL described by Honda et al. (1983) may also lie in this zone. The

→

Figure 9. *A–C*, Anterogradely labeled fibers and terminals emanating from the contralateral spinal trigeminal nucleus and passing near or terminating mainly in the matrix regions of VPM. *A* and *C* are uncounterstained; *B* is counterstained. The borders of nuclei are outlined by *dots* or *dashes* in *A* and *B*. *D* is a CO-stained section adjacent to *C*. The *arrow* in *A* indicates terminal patches at posteromedial pole of VPM. The *arrow* in *B* indicates a terminal cluster in association with the medial aspect of a cluster of large neurons from a CO rod region. Scale bars: 150 μm, *A, C, D*; 100 μm, *B*.

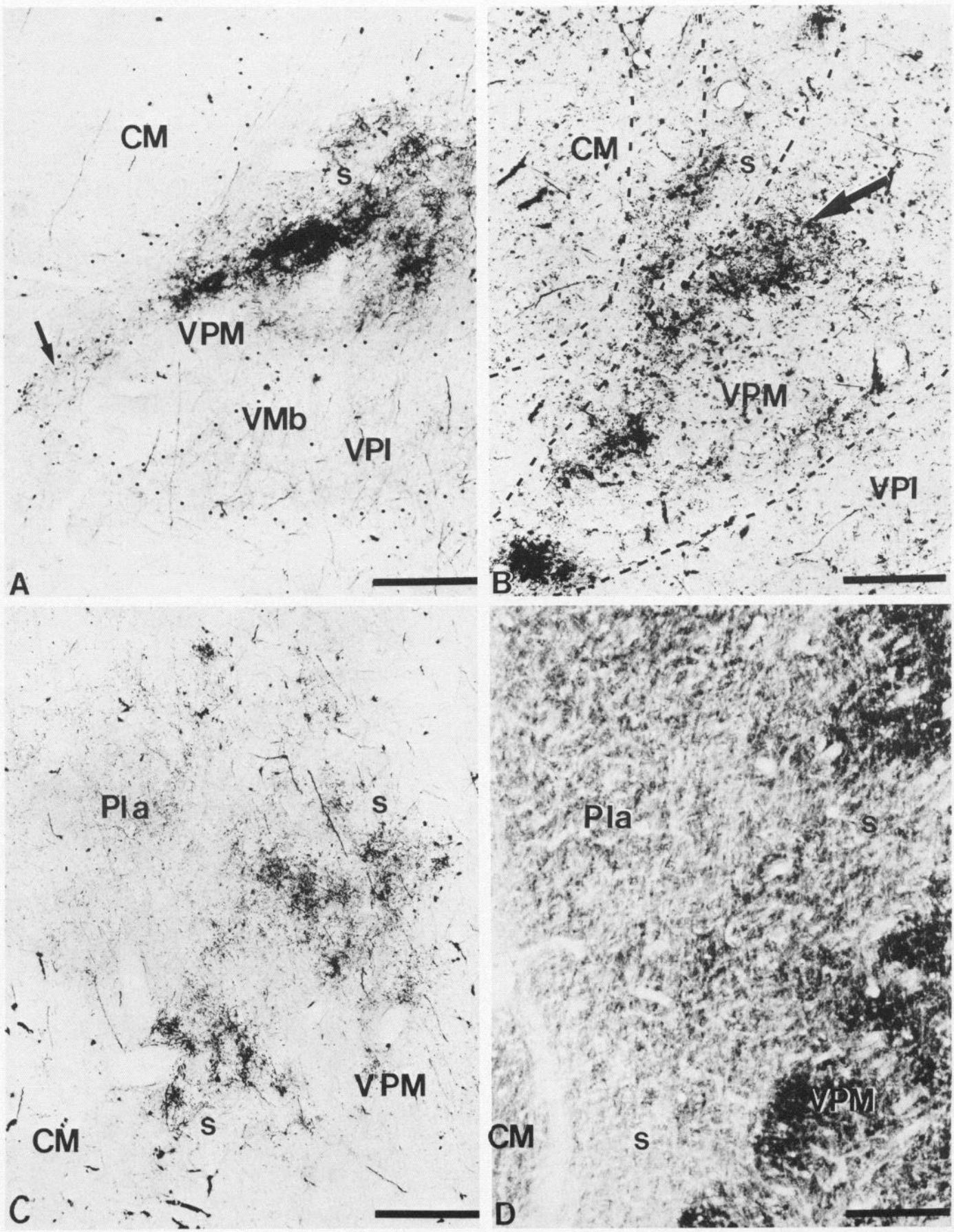
CM
s
VPM
VMb
VPl
A
CM
s
VPM
VPl
B
Pla
s
VPM
CM
s
C
Pla
s
VPM
CM
s
D

matrix zone of the monkey VPM therefore may be found to be the zone that contains nociceptive-responsive cells similar to that reported in the cat and may constitute the principal pain pathway from the head, face, and mouth to the cerebral cortex. Work is in progress to determine if a similar selective innervation of calbindin-positive cells by spinothalamic fibers occurs in VPL.

The 2 populations of cells that characterize the rod and matrix domains of VPM, apart from being of different sizes, chemically distinct, and innervated by different afferent systems, are also distinguished by their differential projections upon the cerebral cortex. The calbindin-positive cells of the matrix compartment clearly project to layer I (and possibly to layer II), while the parvalbumin-positive cells of the rod compartment have heavy projections to deeper layers. The retrograde labeling of matrix cells after deeper injections probably reflects the involvement both of layer I and of fibers passing through the deeper layers to layer I, but it is impossible to rule out that some calbindin cells may project to deeper layers as well as to the most superficial layers. The differential input–output relations of the 2 populations of thalamic cells are still striking. The presence of a population of small VPM cells projecting to layer I is similar to the observations of Penny et al. (1982) and Rausell and Avendaño (1985), who reported a set of small cells in the VPL nucleus projecting to layer I of the cerebral cortex in cats. It will be interesting to determine if a layer I-projecting small-celled population can be detected in the monkey VPL, if the cells comprising it represent the small, calbindin-positive population of the nucleus (Jones and Hendry, 1989; Rausell and Jones, 1991, their Fig. 10), if they lie in the small CO-weak patches seen in that nucleus (E. Rausell and E. G. Jones, unpublished observations), and if there is a differential innervation of these and the larger parvalbumin-positive population by spinothalamic and dorsal column–lemniscal fibers.

The differential projection of parvalbumin- and calbindin-positive cells upon deep and superficial layers of the cerebral cortex, as well as their selective innervation by different sets of afferent fibers, have their parallels in the visual system of monkeys. In the dorsal lateral geniculate nucleus of monkeys, parvalbumin-immunoreactive cells are found predominantly in the principal laminae (1–6), while calbindin-immunoreactive cells are confined to the S laminae and interlaminar zones (Jones and Hendry, 1989). The principal laminae project primarily to subdivisions of layer IV of the visual cortex (Hubel and Wiesel, 1969, 1972), while the S laminae and interlaminar cells appear to project to more superficial layers (I–III; Fitzpatrick et al., 1983). Although data are incomplete for the afferent innervation of the S laminae and interlaminar cells, it is generally considered, largely from analogy with other species, that they are innervated by classes of retinal ganglion cells different from those that innervate the principal laminae (Livingstone and Hubel, 1982). Taken together with the present results, these data suggest that a general principle of thalamic nuclear organization may be emerging in which classes of relay neurons selectively innervated by different components of a sensory system, show differential expression of calcium-binding proteins, and project differentially upon the cerebral cortex. This principle may hold the key to reconciling many discrepant anatomical reports about thalamocortical connectivity, for, as the present results imply, the distribution of the 2 populations may not coincide with the same traditional nuclear boundaries in the thalamus. The calbindin-positive cells of VPM, for example, appear to form part of a more diffusely spread population that has islands in all adjacent nuclei innervated by the spinal trigeminal and spinothalamic systems.

References

Burton H, Craig AD (1979) Distribution of trigeminothalamic projection cells in cat and monkey. Brain Res 161:515–521.

Burton H, Craig AD (1983) Spinothalamic projections in cat, raccoon and monkey: a study based on anterograde transport of horseradish peroxidase. In: Somatosensory integration in the thalamus (Macchi G, Rustioni A, Spreafico A, eds) pp 1–25. Amsterdam: Elsevier.

Chung JM, Surmeier DJ, Lee KH, Sorkin LS, Honda CN, Tsong Y, Willis WD (1986a) Classification of primate spinothalamic and somatosensory thalamic neurons based on cluster analysis. J Neurophysiol 56:308–327.

Chung JM, Lee KH, Surmeier DJ, Sorkin LS, Kim J, Willis WD (1986b) Response charcteristics of neurons in the ventral posterior lateral nucleus of the monkey thalamus. J Neurophysiol 56:370–390.

Craig AD, Burton H (1985) The distribution and topographical organization in the thalamus of anterogradely-transported horseradish peroxidase after spinal injections in cat and raccoon. Exp Brain Res 238:1–28.

Dykes RW (1983) Parallel processing of somatosensory information: a theory. Brain Res Rev 6:47–115.

Fitzpatrick D, Itoh K, Diamond IT (1983) The laminar organization of the lateral geniculate body and the striate cortex in the squirrel monkey (*Saimiri sciureus*). J Neurosci 3:673–702.

Ganchrow D (1978) Intratrigeminal and thalamic projections of nucleus caudalis in the squirrel monkey (*Saimiri sciureus*): a degeneration and autoradiographic study. J Comp Neurol 178:281–312.

Hardy H, Heimer L (1977) A safer and more sensitive substitute for diaminobenzidine in the light microscopic demonstration of retrograde and anterograde axonal transport of HRP. Neurosci Lett 5:235–240.

Honda CN, Perl ER, Mense S (1983) Neurons in ventrobasal region of cat thalamus selectively responsive to noxious mechanical stimulation. J Neurophysiol 49:662–673.

Hubel DH, Wiesel TN (1969) Anatomical demonstration of columns in the monkey striate cortex. Nature 221:747–750.

Hubel DH, Wiesel TN (1972) Laminar and columnar distribution of geniculo-cortical fibers in the macaque monkey. J Comp Neurol 146: 421–450.

Jones EG, Hendry SHC (1989) Differential calcium binding protein immunoreactivity distinguishes classes of relay neurons in monkey thalamic nuclei. Eur J Neurosci 1:222–246.

Jones EG, Friedman DP, Hendry SHC (1982) Thalamic basis of place and modality-specific columns in monkey somatosensory cortex: a correlative anatomical and physiological study. J Neurophysiol 48: 545–568.

Jones EG, Hendry SHC, Brandon C (1986a) Cytochrome oxidase staining reveals functional organization of monkey somatosensory thalamus. Exp Brain Res 62:438–442.

Jones EG, Schwark HD, Callahan PA (1986b) Extent of the ipsilateral representation in the ventral posterior medial nucleus of the monkey thalamus. Exp Brain Res 63:310–320.

Kniffki K-D, Mizumura K (1983) Responses of neurons in VPL and VPL-VL regions of the cat to algesic stimulation of muscle and tendon. J Neurophysiol 49:649–661.

Kniffki K-D, Vahle-Hinz C (1987) The periphery of the cat's ventroposteromedial nucleus (VPMp): nociceptive neurones. In: Thalamus and pain, (Besson JM, Guilbaud G, Peschanski M, eds), pp 245–258. Amsterdam: Elsevier.

Livingstone MS, Hubel DH (1982) Thalamic inputs to cytochrome oxidase-rich regions in monkey visual cortex. Proc Natl Acad Sci USA 779:6098–6106.

Mesulam MM (1978) Tetramethylbenzidine for horseradish peroxidase neurohistochemistry: a noncarcinogenic blue reaction product with superior sensitivity for visualizing neural afferents and efferents. J Histochem Cytochem 26:106–117.

Mountcastle VB (1984) Central nervous mechanisms in mechanoreceptive sensibility. In: Handbook of physiology: the nervous system II (Darian-Smith I, ed), pp. 789–897. Washington, DC: American Physiological Society.

Penny GR, Itoh K, Diamond IT (1982) Cells of different sizes project

to different layers of the somatic cortex in the cat. Brain Res 242:55–65.

Price DD, Dubner, Hu JW (1976) Trigeminothalamic neurons in nucleus caudalis responsive to tactile, thermal, and nociceptive stimulation of monkey's face. J Neurophysiol 39:936–953.

Rausell E, Avendaño C (1985) Thalamo-cortical neurons projecting to superficial and to deep layers in parietal, frontal and prefrontal regions in the cat. Brain Res 347:159–165.

Rausell E, Jones EG (1989) Modular organization of the thalamic VPM nucleus in monkeys. Soc Neurosci Abstr 15:311.

Rausell E, Jones EG (1991) Histochemical and immunocytochemical compartments of the thalamic VPM nucleus in monkeys and their relationship to the representational map. J Neurosci 11:210–225.

Surmeier DJ, Honda CN, Willis WD (1988) Natural groupings of primate spinothalamic neurons based on cutaneous stimulation. Physiological and anatomical features. J Neurophysiol 59:833–860.

Vahle-Hinz C, Freund I, Kniffki K-D (1987) Nociceptive neurons in the ventral periphery of the cat thalamic ventroposteromedial nucleus. In: Fine afferent nerve fibers and pain (Schmidt RF, Vahle-Hinz C, eds) pp 440–450. Weinheim: Edition Medizin.

Willis WD (1987) The spinothalamic tract in primates. In: Thalamus and pain (Besson JM, Guilbaud G, Peschanski M, eds) pp. 35–47. Amsterdam: Elsevier.

Willis WD, Kenshalo DR Jr, Leonard RB (1979) The cells of origin of the primate spinothalamic tract. J Comp Neurol 188:543–574.

Wong-Riley M (1979) Changes in the visual system of monocularly sutured or enucleated cats demonstrable with cytochrome oxidase histochemistry. Brain Res 171:11–28.

Yezierski RP, Sorkin LS, Willis WD (1988) Response properties of spinal neurons projecting to midbrain or midbrain-thalamus in monkey. Brain Res 437:165–170.

Yokota T, Matsumoto N (1983) Location and functional organization of trigeminal wide dynamic range neurons within the nucleus ventralis posteromedialis of the cat. Neurosci Lett 39:231–236.

Yokota T, Koyama N, Matsumoto N (1985) Somatotopic distribution of trigeminal nociceptive neurons in ventrobasal complex of cat thalamus. J Neurophysiol 53:1387–1400.

Yokota T, Asato F, Koyama N, Masuda T, Taguchi H (1988) Nociceptive body representation in nucleus ventralis posterolateralis of cat thalamus. J Neurophysiol 60:1714–1727.